Available online at www.sciencedirect.com
SCIENCE DIRECT®
Pergamon
Materials Research Bulletin 38 (2003) 1767–1772
Materials Research Bulletin
www.elsevier.com/locate/matresbu

X-ray diffraction and Raman scattering in SbSI nanocrystals

A.V. Gomonnai[a], I.M. Voynarovych[b], A.M. Solomon[a], Yu.M. Azhniuk[a,*], A.A. Kikineshi[b], V.P. Pinzenik[b], M. Kis-Varga[c], L. Daroczy[d], V.V. Lopushansky[a]

[a]*Institute of Electron Physics, Ukranian National Academy of Science, Universytetska St. 21, Uzhhorod 88017, Ukraine*
[b]*Uzhhorod National University, Pidhirna St. 46, Uzhhorod 88000, Ukraine*
[c]*Institute of Nuclear Research, Hungarian Academy of Science, P.O. Box 51, Debrecen 4001, Hungary*
[d]*Department of Solid State Physics, University of Debrecen, P.O. Box 2, Debrecen 4010 Hungary*

Received 4 April 2003; received in revised form 7 July 2003; accepted 16 July 2003

Abstract

Lattice structure and rod-like shaped SbSI nanocrystals obtained by ball milling with rod thickness down to 70 nm, as estimated from X-ray diffraction (XRD) and electron microscopy, is similar to that of the bulk crystals. The dependence of the grain size on the milling duration is discussed in view of the chain-like crystalline structure of SbSI. Possible factors, responsible for the observed Raman line broadening, are discussed, scattering by surface phonons being considered the predominant one.

Keywords: A. Inorganic compounds; A. Nanostructures; C. Raman spectroscopy; C. X-ray diffraction

1. Introduction

SbSI is a known ferroelectric material with the phase transition at room temperature (295 K), high dielectric permeability, piesoelectric effect, electrooptical characteristics and photoconductivity making it a promising material for a variety of applications [1]. The studies of nanometric ferroelectrics have shown that their parameters can strongly depend on the crystallite size [2–5]. Therefore obtaining and investigation of SbSI nanocrystals seems interesting for both fundamental and applied physics. As far as we know, so far there has been only a single recent publication on nanocrystalline SbSI, obtained by sol–gel method [6].

* Corresponding author. Tel.: +380-312243822; fax: +380-312243650.
E-mail address: azh@iep.uzhgorod.ua (Yu.M. Azhniuk).

0025-5408/$ – see front matter
doi:10.1016/S0025-5408(03)00181-8

Here we report the results on obtaining SbSI nanocrystals and their characterization by transmission electron microscopy, X-ray diffraction (XRD) and Raman scattering.

2. Experimental

SbSI single crystals were grown by chemical transport, the details of the growth technique being described in [7]. The microcrystalline powders of various grain size were obtained by ball milling the material in a stainless steel cylindrical vial with a hardened steel ball, similar to that described in [8]. A vibrating frame (type Fritsch Pulverisette 0) was used to keep in motion the vial and the ball. Prior to milling the vial was evacuated and then sealed. The 50-h milling process was interrupted after 1-, 2-, 3-, 4-, 5- and 25-h periods and each time a small amount of powder was taken for investigation. The grain size reduction achieved during each milling step was followed by measuring XRD spectra of powders with a horizontal Siemens diffractometer by using Cu $K_{\alpha 1}$ radiation.

For transmission electron microscopy (TEM) investigations the ball-milled powder was mixed with epoxy resin and a thin layer of this mixture was spread between two silicon layers, and this structure was embedded into a 3-mm-diameter aluminium disc. After the epoxy being cured the sample was grinded and polished mechanically from both sides. The final thinning was performed with low-angle ($<5^{\circ}$) Ar-ion treatment. A JEOL 2000 FX-II transmission electron microscope equipped with an Oxford Link-Isis EDS system was used for the TEM measurements.

Raman scattering measurements were performed at room temperature on a LOMO DFS-24 double grating monochromator with a FEU-79 phototube and a photon counting system, the excitation being provided by a He–Ne laser (632.8 nm). The spectral slit did not exceed 1 cm^{-1}.

3. Results and discussion

Fig. 1 illustrates a TEM image of one of the fractions of the obtained SbSI microcrystalline powders from which the shape and average size of the grains can be evaluated. It is clearly seen that the crystallites are of needle-like shape similar to that of bulk SbSI crystals and are quite different from the generally spherical shape of SbSI nanocrystals obtained in [6] by sol–gel method. The formation of the rod-shaped crystallites under milling can be, in our opinion, related to the chain-like crystalline structure of SbSI where four formula units in the unit cell form the elements of two chains with the intrachain forces of ionic and covalent nature and weak van der Waals interchain forces [9].

Mechanical fracture of crystalline materials begins from their breaking down at the defects with minimal strength (macro- and microcracks). Hence, in the course of attrition the strength of the microcrystalline material increases what results in a considerable increase of energy being dissipated for further milling. It is quite reasonable to suppose that the smaller and less deficient crystals will break down more probably in the directions where the van der Waals forces act. That is why the shape of the milled crystallites resembles that of the bulk samples. As seen from the TEM image of Fig. 1, the length of the rod-shaped SbSI crystallites after 50-h milling varied from 0.5 to 1 μm while their thickness was mostly within 50–100 nm.

X-ray diffraction analysis (Fig. 2) has confirmed that SbSI lattice structure is preserved for the nanocrystalline samples. As seen from the figure, the intensities of the diffraction peaks

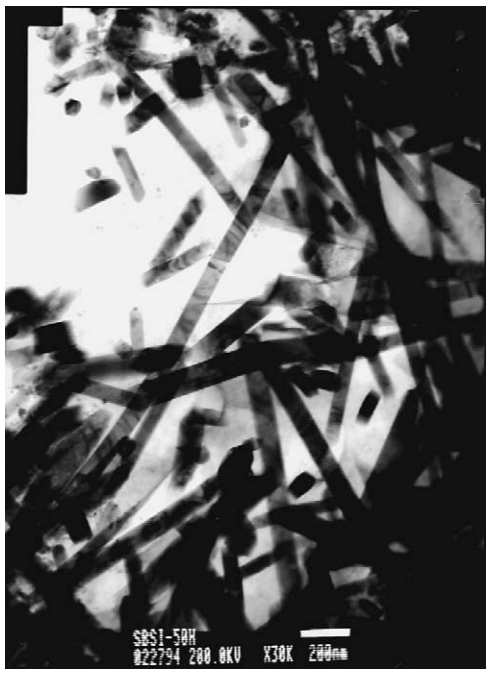

Fig. 1. TEM image of SbSI powder after 50-h milling.

corresponding to the planes parallel to the z axis ((3 1 0), (2 2 0), (1 3 0)) decrease with the milling duration much faster than those for (1 2 1) and (2 1 1) peaks. This indicates that the amount of (h k 0) reflecting planes decreases in the course of milling more rapidly, which is quite consistent with the rod-like shape of the crystallites, observed in Fig. 1. However, in our opinion, the behaviour of the

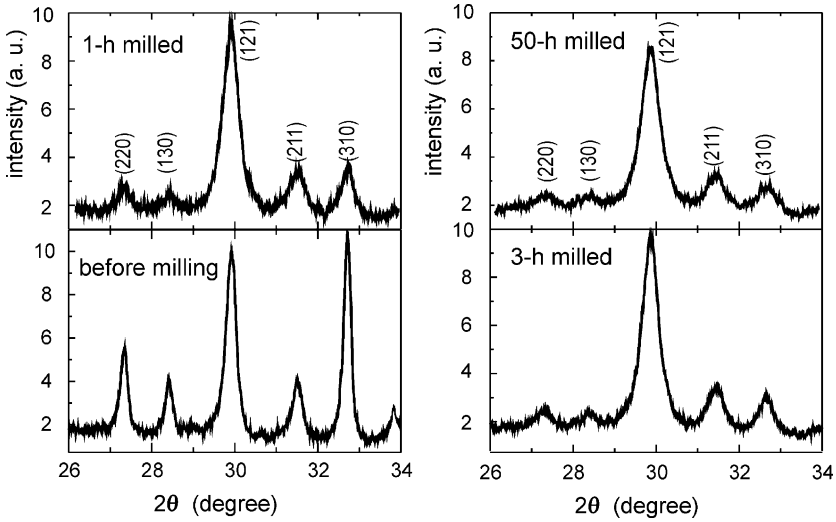

Fig. 2. X-ray diffraction patterns for SbSI micro- and nanocrystals.

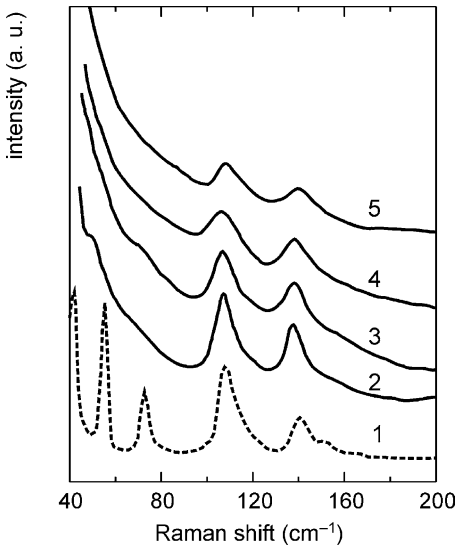

Fig. 3. Raman spectra of SbSI crystallites before milling (curve 2) and after 1-h (curve 3), 3-h (curve 4) and 25-h (curve 5) milling compared with the bulk crystal spectrum, taken from [12] (curve 1).

diffraction peak intensities with the size reduction should not be used for quantitative estimations since no special measures for providing random orientation of the crystallites under measurement have been taken.

With the decrease of $h\ k\ 0$ intensities the diffraction peaks become broader (Fig. 2). The estimation of the crystallite size, which is related to the peak halfwidth [10], have shown that the strongest size reduction occurs during the first hour of milling, and it slows down subsequently.

The measured Raman spectra of nanocrystalline SbSI powders, obtained by milling of different duration, are shown in Fig. 3 along with the bulk crystal spectrum from [11]. As seen from the figure, in the low-frequency range (below 100 cm^{-1}), where for the bulk crystal a rich phonon spectrum is reported [11–13] (curve 1), in the spectra of powder samples the phonon bands are smeared, being masked in the Rayleigh scattering wing, the intensity of the latter increasing with the size reduction. Only for microcrystalline powders (curve 2) and the first nanometric powder fraction (curve 3) some features in the low-frequency range can be detected. Meanwhile the Raman bands at 107 and 139 cm^{-1} are clearly observed for all nanometric samples. It should be noted that the frequencies of the discussed two bands are practically independent of the milling duration, i.e. of the nanocrystal size, while their halfwidths, estimated after Rayleigh wing constituent having been subtracted, appear to grow continuously in the course of the milling what is illustrated by Fig. 4.

Such behaviour of Raman band parameters on the crystallite size is rather typical for semiconductor microcrystals whose Raman spectra were thoroughly studied, e.g. for Si [14,15], GaP [14], $CdS_{1-x}Se_x$ [16,17]. It should be noted that, contrary to our case, in most cases the size decrease-induced broadening is accompanied by slight downward shift of the peak frequencies and Raman band asymmetry with a more pronounced low-frequency wing. Generally the observed features are most often explained by confinement-related selection rules relaxation due to the small crystallite size [15–18] and surface phonon modes [16,19,20].

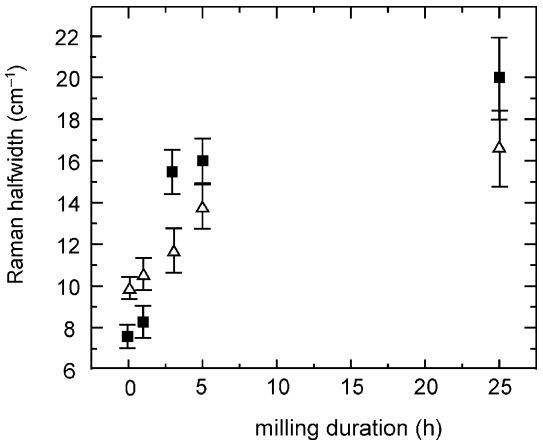

Fig. 4. Raman halfwidth dependence for SbSI crystallites on the milling duration for the bands centred at 107 cm^{-1} (open triangles) and 139 cm^{-1} (solid squares).

We have estimated the confinement-related contribution into the Raman line broadening and asymmetry for the observed Raman bands with the nanocrystal size decrease. The calculations have shown that such effects can be revealed only if the size parameters are reduced to 5–10 nm, which is much smaller than the nanocrystals under investigation. Hence, the observed Raman line broadening should be explained by surface phonon modes.

The theory of surface phonon modes, arising in crystals due to the finiteness of their size, is well elaborated, especially for ferroelectrics [21]. Due to the size decrease in nanocrystals the surface-to-bulk contribution ratio into the Raman spectrum is much higher than in bulk crystals. Therefore, one might expect Raman observation of Fröhlich surface phonon modes [19] whose frequencies are usually somewhat below those for the corresponding longitudinal bulk phonons while the surface phonons bands being considerably broader. Since in our case the frequencies of the discussed phonon modes are only slightly above 100 cm^{-1}, the shift of the band frequency due to the increase of the surface phonon contribution could hardly be detected. However, the broadening of the Raman lines by factor of about 2 in the course of milling is quite consistent with the increase of the surface-to-bulk ratio.

4. Conclusions

Nanometric needle-like crystals of SbSI were obtained by milling, their shape and average size was determined from TEM measurements. X-ray diffraction studies have shown that the decrease of SbSI grain size is much slowed down after the first hour of milling. The average transverse size of the crystallites of about 100 nm was achieved. This fact is related to the chain-like crystalline structure of SbSI and the difference in the nature of the interchain and intrachain forces. In the Raman spectra of SbSI nanocrystals with the average width down to ~70 nm, the bands at 107 and 139 cm^{-1} are observed; their broadening with the size decrease is discussed in view of phonon confinement-related selection rule relaxations and scattering by surface phonons. Based on calculations, the former factor is considered to be negligible in comparison with the surface phonons contribution.

References

[1] E. Fatuzzo, G. Harbeke, W.J. Merz, R. Nitzsche, H. Roetschi, W. Ruppel, Phys. Rev. 127 (1962) 2036.
[2] T. Kanata, T. Yoshikawa, K. Kubota, Solid State Commun. 62 (1987) 765.
[3] K. Ishikawa, K. Yoshikawa, N. Okada, Phys. Rev. B. 37 (1988) 5852.
[4] W.L. Zhong, Y.G. Wang, P.L. Zhang, B.D. Qu, Phys. Rev. B. 50 (1994) 698.
[5] D.-L. Yao, Y.-Z. Wu, Z.-Y. Li, Phys. Stat. Sol. B 231 (2002) 3.
[6] Y. Xu, F. Del Monte, J.D. Mackenzie, K. Namjoshi, P. Muggli, C. Joshi, Ferroelectrics 230 (1999) 11.
[7] L.M. Belyayev, L.A. Lyakovitskaya, G.V. Netesov, Neorganicheskie Materialy 1 (1965) 2178.
[8] H. Bakker, L.M. Di, D.M.R. Lo Cascio, Solid State Phenomena 23-24 (1992) 253.
[9] Y. Yomada, H. Chihara, J. Phys. Soc. Jap. 21 (1966) 327.
[10] A. Guinier. Théorie et technique de la radiocristallographie, 2nd ed., Paris, Dunod, 1956.
[11] M. Balkanski, M.K. Teng, S.M. Shapiro, M.K. Ziolkiewicz, Phys. Stat. Sol. B 44 (1971) 355.
[12] D.K. Agrawal, C.H. Perry, Phys. Rev. B 4 (1971) 1893.
[13] E. Furman, O. Brafman, J. Makovsky, Phys. Rev. B 8 (1973) 2341.
[14] S. Hayashi, K. Yamamoto, Superlattices Microstruct. 2 (1986) 581.
[15] P.M. Fauchet, I.H. Campbell, Crit. Rev. Solid State Mater. Sci. 14 (1988) S79.
[16] A. Roy, A.K. Sood, Phys. Rev. B 53 (1996) 12127.
[17] A. Ingale, K.C. Rustagi, Phys. Rev. B 58 (1998) 7197.
[18] C. Trallero-Giner, A. Debernardi, M. Cardona, E. Menendez-Proupin, A.I. Ekimov, Phys. Rev. B 57 (1998) 4664.
[19] S. Hayashi, R. Ruppin, J. Phys. C: Solid State Phys. 18 (1985) 2583.
[20] Y.N. Hwang, S.H. Park, D. Kim, Phys. Rev. B 59 (1999) 7285.
[21] M.G. Cottam, D.R. Tilley, B. Žekš, J. Phys. C: Solid State Phys. 17 (1984) 1793.